

## Article

# Measurement of Multi-Stokes Ultrashort Pulse Shapes of Synchronously Pumped Stimulated Raman Scattering on Combined Vibrational Modes in a BaWO<sub>4</sub> Crystal

Dmitry P. Tereshchenko<sup>1</sup>, Egor A. Peganov<sup>2</sup>, Sergei N. Smetanin<sup>1,\*</sup> , Alexander G. Papashvili<sup>1</sup>, Evgeny V. Shashkov<sup>1</sup>, Lyudmila I. Ivleva<sup>1</sup>, Elizaveta E. Dunaeva<sup>1</sup> , Irina S. Voronina<sup>1</sup> and Milan Frank<sup>3</sup> 

<sup>1</sup> Research Center for Laser Materials and Technologies, Prokhorov General Physics Institute of the Russian Academy of Sciences, Vavilova 38, 119991 Moscow, Russia; tereshchenko.mitya2018@yandex.ru (D.P.T.); aleks-papa@mail.ru (A.G.P.); shashkov@kapella.gpi.ru (E.V.S.); ivleva@lst.gpi.ru (L.I.I.); edunaeva@lst.gpi.ru (E.E.D.); irina.voronina.78@list.ru (I.S.V.)

<sup>2</sup> College of New Materials and Nanotechnologies, National University of Science and Technology MISiS, Leninski Prospekt 4, 119049 Moscow, Russia; eapeganov@yandex.ru

<sup>3</sup> Faculty of Nuclear Sciences and Physical Engineering, Czech Technical University, Břehová 7, 11519 Prague, Czech Republic; frankmil@fjfi.cvut.cz

\* Correspondence: ssmetanin@bk.ru



**Citation:** Tereshchenko, D.P.; Peganov, E.A.; Smetanin, S.N.; Papashvili, A.G.; Shashkov, E.V.; Ivleva, L.I.; Dunaeva, E.E.; Voronina, I.S.; Frank, M. Measurement of Multi-Stokes Ultrashort Pulse Shapes of Synchronously Pumped Stimulated Raman Scattering on Combined Vibrational Modes in a BaWO<sub>4</sub> Crystal. *Crystals* **2022**, *12*, 495. <https://doi.org/10.3390/cryst12040495>

Academic Editors: Ram S. Katiyar and Sergio Brutti

Received: 27 February 2022

Accepted: 31 March 2022

Published: 2 April 2022

**Publisher's Note:** MDPI stays neutral with regard to jurisdictional claims in published maps and institutional affiliations.



**Copyright:** © 2022 by the authors. Licensee MDPI, Basel, Switzerland. This article is an open access article distributed under the terms and conditions of the Creative Commons Attribution (CC BY) license (<https://creativecommons.org/licenses/by/4.0/>).

**Abstract:** Multi-Stokes ultrashort pulse shapes and their relative positions of synchronously pumped stimulated Raman scattering (SRS) on combined primary and secondary vibrational modes in a BaWO<sub>4</sub> crystal are investigated. An original method of its simultaneous measurement with the help of a streak camera has been developed. The structure of SRS pulses at the pulse shortening effect down to the pulse duration, close to the dephasing time of the secondary Raman mode of the BaWO<sub>4</sub> crystal, is registered and analyzed for the detuning of the Raman laser cavity length.

**Keywords:** Raman crystal; synchronous pumping; combined Raman modes; pulse shortening

## 1. Introduction

Crystalline Raman lasers are reliable sources of coherent radiation at wavelengths inaccessible to conventional lasers. According to the magnitude of the Raman gain ( $g$ ), barium tungstate (BaWO<sub>4</sub>) crystals ( $g = 8.5$  cm/GW at the Raman shift of  $925$  cm<sup>-1</sup> under  $1.06$   $\mu$ m pumping [1]) are among the top three active crystals for Raman lasers, along with CVD-diamond ( $g = 17$  cm/GW at the Raman shift of  $1333$  cm<sup>-1</sup> under  $1.06$   $\mu$ m pumping [2]) and Ba(NO<sub>3</sub>)<sub>2</sub> ( $g = 11$  cm/GW at the Raman shift of  $1047$  cm<sup>-1</sup> under  $1.06$   $\mu$ m pumping [1]). Moreover, unlike them but similar to the other tetragonal crystals, BaWO<sub>4</sub> has not only one, but two (primary and secondary) intense lines in a spontaneous Raman spectrum. These lines in BaWO<sub>4</sub> correspond to stretching (wavenumber  $\nu_1 = 925$  cm<sup>-1</sup>, linewidth  $\Delta\nu_1 = 1.6$  cm<sup>-1</sup>) and bending (wavenumber  $\nu_2 = 332$  cm<sup>-1</sup>, linewidth  $\Delta\nu_2 = 3.8$  cm<sup>-1</sup>) modes of internal vibrations of anionic groups [3]. It was in BaWO<sub>4</sub> that stimulated Raman scattering (SRS) with a combined frequency shift of  $\nu_1 + \nu_2$  was previously observed for the first time [4]. After that, similar effects were studied for many other crystals having a lower Raman gain, including KGd(WO<sub>4</sub>)<sub>2</sub>, GdVO<sub>4</sub>, YVO<sub>4</sub>, SrWO<sub>4</sub>, SrMoO<sub>4</sub>, Ca<sub>3</sub>(VO<sub>4</sub>)<sub>2</sub>, PbMoO<sub>4</sub>, and Pb(MoO<sub>4</sub>)<sub>0.2</sub>(WO<sub>4</sub>)<sub>0.8</sub> [5–11]. These effects were experimentally realized in schemes of Raman lasers with a high-Q optical cavity compensating a lower Raman gain at the secondary Raman mode rather than at the primary Raman mode. In the case of ultrashort pulse pumping, the method [12] of synchronous pumping by repetitive laser pulses with a repetition period synchronized with the Raman laser cavity round-trip time was used. Synchronously pumped SRS with the combined frequency shift was realized for the first time again in a high-gain BaWO<sub>4</sub> crystal using linear [13] and ring [14] optical cavities, and then in other crystals [8–11]. The interest in such synchronously pumped

crystalline Raman lasers is due to the observed phenomenon of the strong shortening of SRS pulses with a combined frequency shift down to the dephasing time  $\tau_2 = 1/(\pi c \Delta\nu_2)$  of the secondary Raman mode. Therefore, the SRS pulse duration becomes shorter than the primary Raman mode dephasing time  $\tau_1 = 1/(\pi c \Delta\nu_1)$ , and it amounts  $\sim 1$  ps and shorter under pumping by 36 ps pulses [8–11,13,14]. This phenomenon so far has only a qualitative explanation as a combination of several optical effects. It can be explained not only by the combination of effects of group velocity walk-off and strong pump pulse depletion [15,16] (it was studied only for the first Stokes pulse), but also by the formation of ultrashort SRS pulses under intracavity excitation [17]. The latter should cause strong shortening of the second Stokes pulse with a combined  $(\nu_1 + \nu_2)$  frequency shift under intracavity pumping by the first  $\nu_1$ -shifted Stokes component. However, in [13], it was also shown that the intracavity oscillated second Stokes component with the primary Raman mode double shift  $(\nu_1 + \nu_1)$ , like the first  $\nu_1$ -shifted Stokes component in BaWO<sub>4</sub>, had no such strong pulse shortening. Therefore, the combined Raman shift is apparently fundamental to obtain strong pulse shortening under synchronous pumping. A study of the pulse shortening mechanism requires simultaneous measurement of not only the durations, but also of the shapes and relative positions of the pulses of different Stokes components. Such a study can be carried out using a streak camera, but in previous works the laser pulse energies ( $\sim 300$  nJ) were not sufficiently high for this.

In the present work, we used the pump 1079 nm, 64 ps Nd:YAP laser with a 1000 times higher pulse energy of 300  $\mu$ J for the experimental study of the output of multi-Stokes ultrashort pulse shapes of the synchronously pumped Raman laser on combined vibrational modes in a BaWO<sub>4</sub> crystal. An original method of simultaneous measurement of pulse shapes and relative temporal positions of several Stokes components of the Raman laser with the help of a streak camera was developed.

## 2. Experimental Setup

The experimental setup of the synchronously pumped Raman laser with the system of measurement of the individual pulse shapes and relative temporal positions for the multi-Stokes output laser radiation is shown in Figure 1.

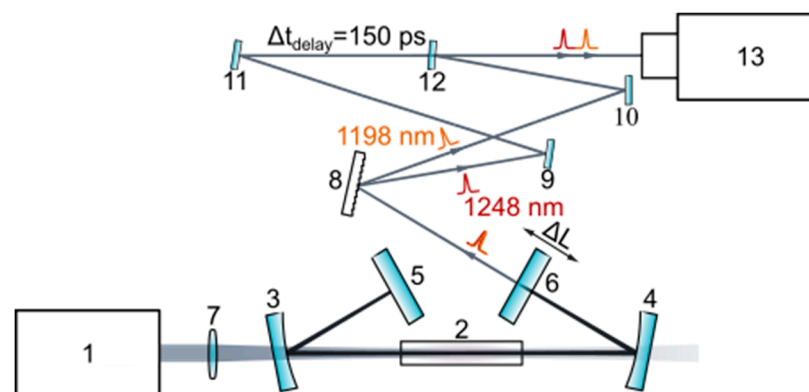


Figure 1. Experimental setup.

The laboratory-designed master oscillator power amplifier Nd:YAP laser system, at a wavelength of  $\lambda_0 = 1079$  nm, was used as the pump laser (1) [18]. The pump laser master oscillator operated in a hybrid mode-locking regime with a passive negative feedback element based on a GaAs crystal [19] to form a long laser pulse train of  $\sim 200$  pulses. The Pockels cell-based pulse extraction system controlled by signals from the DG645 digital delay generator (Stanford Research Systems, Sunnyvale, CA, USA) provided the extraction of a laser pulse train of 56 pulses. It also allowed obtaining equal durations of pulses of  $7 \pm 0.5$  ps at a repetition period of 8 ns in the 56 pulses train. The laser pulse train was directed to a volume Bragg grating [20] with a period varying linearly along the light

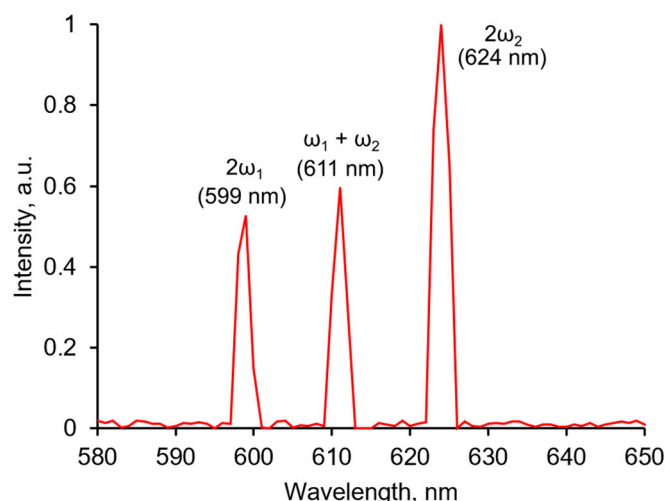
propagation direction. As a result, the laser pulses reflected by the volume Bragg grating were negatively chirped and stretched in time from  $7 \pm 0.5$  ps up to  $64 \pm 4.5$  ps. Then, the chirped laser pulse train was directed to a four-stage amplifier system based on Nd:YAP crystals, increasing the individual, 64 ps, 1079 nm pulse energy up to 300  $\mu$ J. The pump laser system was isolated from the Raman laser under study using a Faraday isolator.

The *a*-cut 43 mm-long BaWO<sub>4</sub> crystal (2), grown by the Czochralski technique at Prokhorov General Physics Institute of the Russian Academy of Sciences, was used as the Raman-active medium. The crystal had no antireflection coatings. The crystal's optical axis (*c*) was oriented for pumping at  $E \parallel c$ , enabling the access of the maximum intensities of both the  $\nu_1$  and  $\nu_2$  Raman modes [8]. The BaWO<sub>4</sub> crystal was placed in an external linear (*z*-fold) cavity with a round-trip time synchronized with the pump pulse repetition period (8 ns) by tuning the Raman laser cavity length. The Raman laser cavity consisted of two concave mirrors (3 and 4) and two flat mirrors (5 and 6). The concave (a curvature radius of  $r = 500$  mm) mirrors had high reflection for the SRS radiation at wavelengths in a range of 1198–1248 nm and high transmission for the pump radiation (1079 nm) and for the SRS components with wavelengths longer than 1248 nm. One of the flat mirrors (5) had high reflection, at 1198–1248 nm. The second (6) was an output coupler with a reflectivity of  $R_{1198} = 99.5\%$  at the 1198 nm and  $R_{1248} = 96\%$  at 1248 nm, and with high transmission for longer wavelength SRS components. It was placed on a precise translation stage for the tuning of the Raman laser cavity length ( $\Delta L$ ). The pump radiation was focused by a lens (7) with a focal length of 1.2 m into the BaWO<sub>4</sub> crystal to a spot with a radius of 300  $\mu$ m, matched with the Raman laser cavity mode.

The measurement system was installed at the laser output behind the output coupler (6). To measure different characteristics of the output laser radiation, we used different tools of measurement (spectrometer, oscilloscope, streak-camera, etc.). Figure 1 shows only the most important system, measuring the laser pulse shapes and its relative temporal positions. The scheme of simultaneous streaking of two light sources used earlier, for example, for electron-beam diagnostics studies [21], was refined here for the characterization of a one multiwavelength Raman laser. To perform this, the output radiation of the Raman laser was split into Stokes components (1198 nm and 1248 nm) by a reflective diffraction grating (8); a system of mirrors (9–11), which formed a delay line ( $\Delta t_{\text{delay}} = 150$  ps); and a semi-transmitting mirror (12), which combined the Stokes components into one beam for measurement by the PS-1/S1 streak camera (13) with a time resolution of 1.5 ps, developed at the Prokhorov General Physics Institute of the Russian Academy of Sciences, Russia [22].

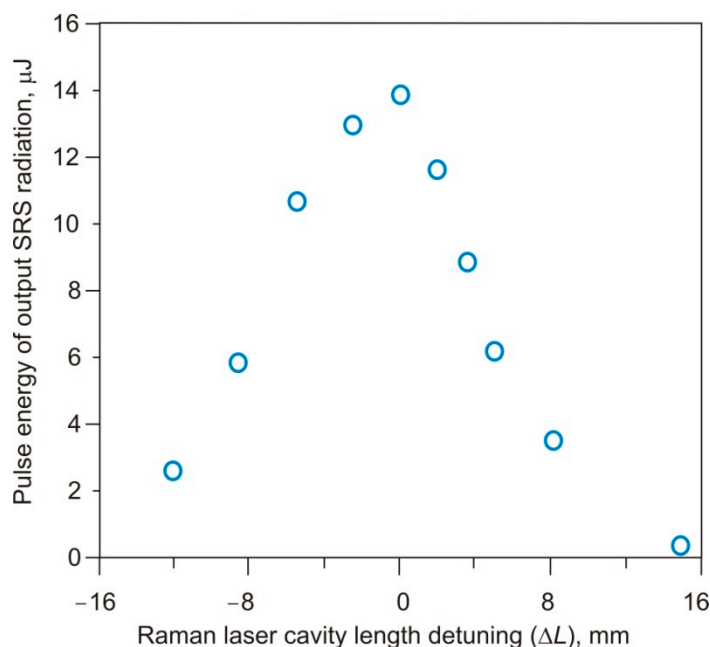
### 3. Experimental Results

Initially, we visualized the output SRS radiation and registered its spectrum. We focused the output SRS radiation using a lens with a focal length of 10 cm into a frequency doubler based on a LiIO<sub>3</sub> crystal (having low difference of phase-matching angles of  $2.9^\circ$  for frequency doubling of the radiations at 1198 and 1248 nm), and we registered the converted visible radiation using the spectrometer Ocean Optics HR2000 (wavelength range 200–1100 nm, resolution  $<2$  nm) (Ocean Insight, Orlando, FL, USA). Figure 2 demonstrates the characteristic registration result. We can see three spectral lines in an orange-red spectral range. The 599 nm and 624 nm lines can be identified as the second harmonics of the first  $\nu_1$ -shifted Stokes SRS component at a wavelength of  $\lambda_1 = (\lambda_0^{-1} - \nu_1)^{-1} = 1198$  nm and the second Stokes SRS component with the combined ( $\nu_1 + \nu_2$ ) frequency shift at a wavelength of  $\lambda_2 = [\lambda_0^{-1} - (\nu_1 + \nu_2)]^{-1} = 1248$  nm, respectively. The intermediate 611 nm line does not correspond to any other SRS component, but it is a sum frequency from the first and second Stokes SRS components. Generation of higher order SRS components with longer wavelengths did not occur because of the selectivity of the Raman laser cavity.



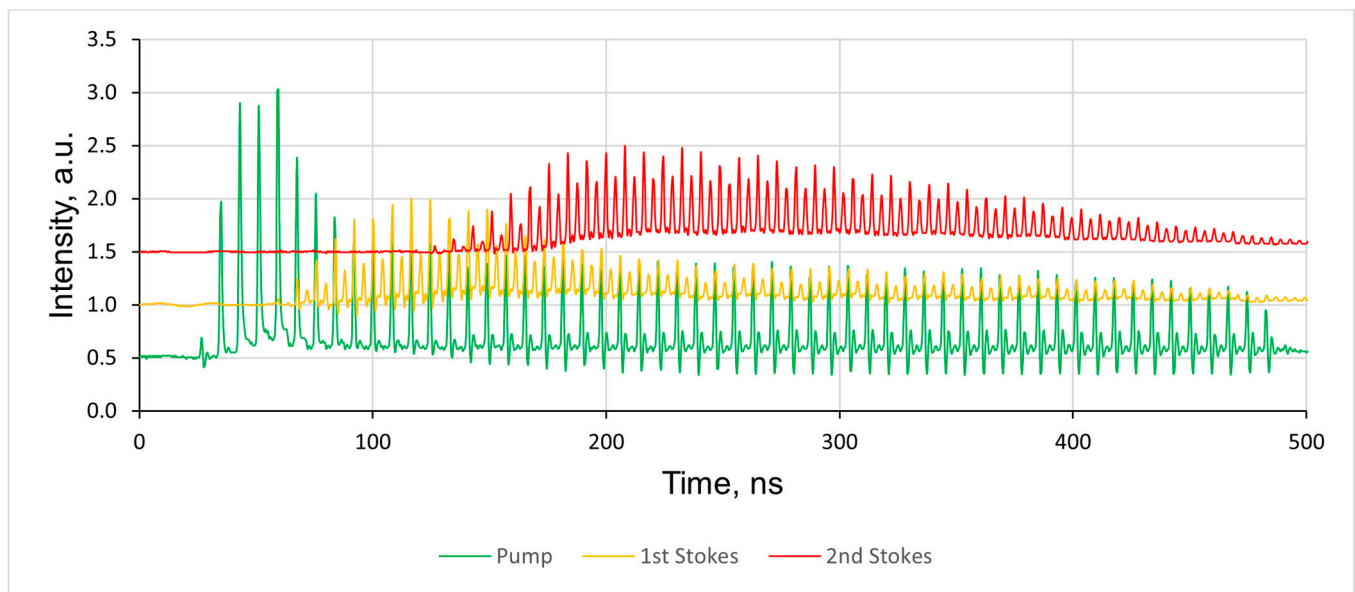
**Figure 2.** Spectrum of the output SRS radiation converted by a  $\text{LiIO}_3$  crystal.

Figure 3 demonstrates the results of detuning the Raman laser cavity length ( $\Delta L$ ). We should note that the detuning curve is more symmetric than for the cases of low-intensity synchronous pumping, in which positive detuning is more critical than negative ones [13,15], and the detuning scale is an order of magnitude wider. We obtained the same character of detuning as in [23], in which similar conditions of high-intensity synchronous pumping were realized for a  $\text{LiIO}_3$  crystal. In Figure 3, zero detuning corresponds to a maximum pulse energy of the output SRS radiation of 14  $\mu\text{J}$  (12% at 1198 nm and 88% at 1248 nm) at a conversion efficiency of 4.7% (the input pump pulse energy was 300  $\mu\text{J}$ ). Pulse energy was measured by the energy meter StarLite (Ophir-Spiricon, LLC, North Logan, UT, USA).



**Figure 3.** Detuning of the Raman laser cavity length.

Then, shapes of the laser pulse trains were recorded using three avalanche photodiodes separately for each laser radiation component (including the residual 1079 nm pump behind the mirror (4) in Figure 1) and displayed on a four-channel oscilloscope LeCroy WaveSurfer 3054 (bandwidth 500 MHz) (Teledyne LeCroy, Inc., Milpitas, CA, USA). The characteristic result is shown in Figure 4.



**Figure 4.** Oscillograms of output radiation components: (green) 1079 nm pump, (yellow) 1198 nm first Stokes, and (red) 1248 nm second Stokes pulse trains.

It can be seen from Figure 4 that cascade-like SRS conversion occurred firstly from the pump (green line) into the first Stokes SRS component (yellow line), and secondly from the first Stokes into the second Stokes SRS component (red line), which is usual. However, SRS radiation pulse trains (yellow and red lines) have a pulse repetition rate that doubles in comparison with that of the pump pulse train (green line). This is unusual and has not previously been observed in synchronously pumped Raman lasers. More precisely, the double repetition rate SRS pulse train consists of two sub-trains with the 8 ns pulse period. The first sub-train (in yellow or red line) is synchronous with the pump pulse train (green line) and has higher intense pulses. The second sub-train is delayed by half of the 8 ns period and has less intense pulses. In the first Stokes pulse train (yellow line), the second sub-train has an intensity of pulses of about 50% of the first sub-train pulse intensity. In the second Stokes pulse train (red line), the second sub-train intensity is even higher—about 70% of the first sub-train pulse intensity. The second sub-train can be explained by backward SRS in addition to forward SRS in the first sub-train. Therefore, a higher intensity of backward SRS at the second Stokes pulse train compared to that of the first Stokes pulse train is caused by intense multi-pass intracavity pumping of the second Stokes oscillation by the first Stokes component, in contrast to single-pass pumping of the first Stokes oscillation.

The reason for the observation of synchronously pumped backward SRS in BaWO<sub>4</sub> can be that the pump pulse duration has a 3.3 times higher ratio compared to the crystal transit time (it is critical for stimulated backscattering [24]) and that it has an order of magnitude of greater intensity of pump pulses (SRS oscillation threshold takes place already at the fourth pulse of the pump pulse train in Figure 4) in comparison with previous similar works with BaWO<sub>4</sub> [13,14].

Figure 5 demonstrates the individual SRS pulse shapes and their relative positions measured with the help of the streak camera at various values of detuning of the Raman laser cavity length. The demonstrated picture was synchronous with the 36th pump pulse in the pump pulse train (Figure 4), and it corresponded to the forward SRS sub-train.

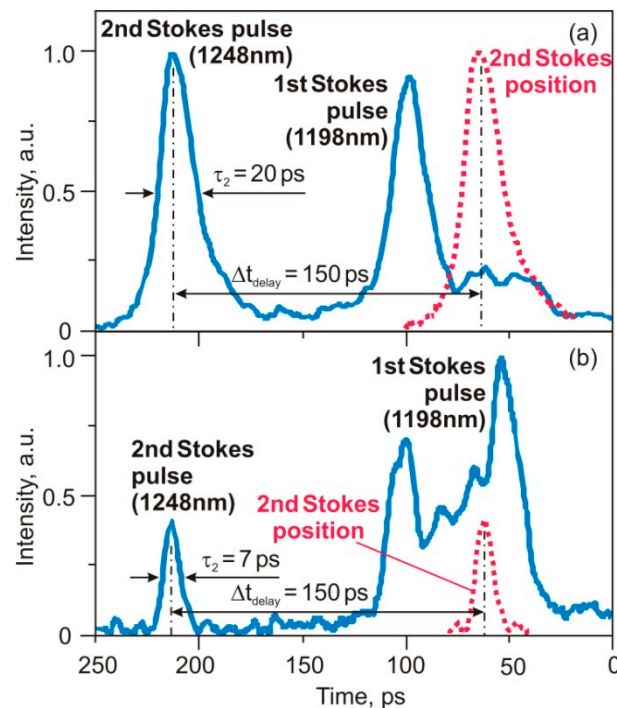


**Figure 5.** Individual SRS pulse shapes and relative positions measured by a streak camera at (a) zero detuning and (b) +8 mm detuning of the Raman laser cavity length.

As one can see from Figure 5a, the zero detuning case corresponds to efficient conversion into the 1248 nm second Stokes component with a combined frequency shift at the pulse duration of  $\tau_2 = 20$  ps and strong depletion of the 1198 nm first Stokes pulse. The first Stokes pulse depletion took place at its leading edge. This can be explained by higher group velocity for the second Stokes component compared to the first Stokes component due to positive dispersion of the active crystal.

It can be seen from Figure 5b that positive detuning ( $\Delta L = +8$  mm) of the Raman laser cavity length led to strong shortening of the second Stokes component with a combined frequency shift down to  $\tau_2 = 7$  ps. This agrees with previous works [13,14]. At this point, the structure of pulses at the shortening effect can be observed. The depleted part of the first Stokes pulse is longer than the second Stokes pulse duration because the second Stokes pulse has a higher group velocity moving to the leading edge of the first Stokes pulse during the multi-pass oscillation process.

Increasing the cavity length detuning from 0 (maximum conversion) up to 15 mm (conversion close to 0) resulted in shortening of the 1248 nm second Stokes pulses from 20 ps down to 4 ps (close to inverse linewidth of secondary Raman mode of BaWO<sub>4</sub> [3]) for keeping the Gaussian shape, as can be seen in Figure 5 with decreasing conversion efficiency due to temporal walk-off between the pump, the first Stokes pulse, and the second Stokes pulse. We should also note that the shortened pulse duration is comparable with the initial pulse duration (7 ps) of the pump laser master oscillator. Therefore, an additional reason for pulse shortening at the negatively chirped pumping is that this chirp compensates by positive dispersion of the BaWO<sub>4</sub> crystal in conditions of multi-pass SRS oscillation. Earlier, in theoretical works [15,16], the effect of shortening a first Stokes pulse in synchronously pumped Raman lasers for positive cavity length detuning was explained by a delay of the first Stokes pulse relative to the pump pulse when the cavity round-trip time was longer than the pump pulse repetition period. Now, we can observe (Figure 5b) a stronger shortening effect for the second ( $\nu_1 + \nu_2$ )-shifted Stokes pulse under intracavity pumping by the first  $\nu_1$ -shifted Stokes pulse. It can be additionally explained by the mechanism of ultrashort pulse formation under intracavity pumping, as predicted in another theoretical work [17].

#### 4. Conclusions

In conclusion, multi-Stokes ultrashort pulse shapes and their relative positions of synchronously pumped stimulated Raman scattering on combined vibrational modes in a BaWO<sub>4</sub> crystal were investigated. The SRS pulse's structure at the pulse shortening effect down to the dephasing time of the secondary Raman mode of the BaWO<sub>4</sub> crystal was registered and analyzed for the detuning of the Raman laser cavity length. The information obtained opens new possibilities for explaining the mechanism of pulse shortening in ultrafast synchronously pumped crystalline Raman lasers and can be used in future works.

**Author Contributions:** Conceptualization, S.N.S.; methodology, M.F. and S.N.S.; software, E.V.S.; validation, A.G.P. and D.P.T.; formal analysis, M.F., D.P.T. and S.N.S.; investigation, D.P.T., E.A.P., S.N.S. and A.G.P.; resources, E.V.S., L.I.I., E.E.D. and I.S.V.; data curation, S.N.S. and M.F.; writing—original draft preparation, S.N.S. and D.P.T.; writing—review and editing, S.N.S. and M.F.; visualization, D.P.T.; supervision, S.N.S. All authors have read and agreed to the published version of the manuscript.

**Funding:** This research was funded by the Russian Science Foundation—Project No 22-22-00708 (<https://rscf.ru/project/22-22-00708/>).

**Institutional Review Board Statement:** Not applicable.

**Informed Consent Statement:** Not applicable.

**Data Availability Statement:** Not applicable.

**Conflicts of Interest:** The authors declare no conflict of interest.

#### References

1. Basiev, T.T.; Osiko, V.V.; Prokhorov, A.M.; Dianov, E.M. Crystalline and Fiber Raman Lasers. In *Solid-State Mid-Infrared Laser Sources*; Sorokina, I.T., Vodopyanov, K.L., Eds.; Springer: Berlin/Heidelberg, Germany, 2003; Volume 89, pp. 359–408.
2. Savitski, V.G.; Reilly, S.; Kemp, A.J. Steady-state Raman gain in diamond as a function of pump wavelength. *IEEE J. Quantum Electron.* **2013**, *49*, 218–223. [[CrossRef](#)]
3. Basiev, T.T.; Sobol, A.A.; Voronko, Y.K.; Zverev, P.G. Spontaneous Raman spectroscopy of tungstate and molybdate crystals for Raman lasers. *Opt. Mater.* **2000**, *15*, 205–216. [[CrossRef](#)]
4. Zverev, P.G.; Basiev, T.T.; Sobol, A.A.; Ermakov, I.V.; Gellerman, W. BaWO<sub>4</sub> crystal for quasi-cw yellow Raman laser. *OSA TOPS* **2001**, *50*, 212–217.
5. Mildren, R.P.; Piper, J.A. Increased wavelength options in the visible and ultraviolet for Raman lasers operating on dual Raman modes. *Opt. Express* **2008**, *16*, 3261–3272. [[CrossRef](#)] [[PubMed](#)]
6. Lin, J.; Pask, H.M. Cascaded self-Raman lasers based on 382 cm<sup>-1</sup> shift in Nd:GdVO<sub>4</sub>. *Opt. Express* **2012**, *20*, 15180–15185. [[CrossRef](#)] [[PubMed](#)]
7. Lin, H.Y.; Pan, X.; Huang, X.H.; Xiao, M.; Liu, X.; Sun, D.; Zhu, W.Z. Multi-wavelength passively Q-switched c-cut Nd:YVO<sub>4</sub> self-Raman laser with Cr<sup>4+</sup>:YAG saturable absorber. *Opt. Commun.* **2016**, *368*, 39–42. [[CrossRef](#)]
8. Frank, M.; Smetanin, S.N.; Jelínek, M.; Vyhlídal, D.; Shukshin, V.E.; Ivleva, L.I.; Dunaeva, E.E.; Voronina, I.S.; Zverev, P.G.; Kubeček, V. Stimulated Raman scattering in alkali-earth tungstate and molybdate crystals at both stretching and bending Raman modes under synchronous picosecond pumping with multiple pulse shortening down to 1 ps. *Crystals* **2019**, *9*, 167. [[CrossRef](#)]
9. Frank, M.; Smetanin, S.N.; Jelínek, M.; Vyhlídal, D.; Ivleva, L.I.; Dunaeva, E.E.; Voronina, I.S.; Tereshchenko, D.P.; Shukshin, V.E.; Zverev, P.G.; et al. Stimulated Raman scattering in yttrium, gadolinium, and calcium orthovanadate crystals with single and combined frequency shifts under synchronous picosecond pumping for sub-picosecond or multi-wavelength generation around 1.2 μm. *Crystals* **2020**, *10*, 871. [[CrossRef](#)]
10. Frank, M.; Smetanin, S.N.; Jelínek, M.; Vyhlídal, D.; Shukshin, V.E.; Zverev, P.G.; Kubeček, V. Highly-efficient, high-energy, picosecond, synchronously pumped Raman laser at 1171 and 1217 nm based on PbMoO<sub>4</sub> crystals with single and combined Raman shifts. *Opt. Express* **2020**, *28*, 39944–39955. [[CrossRef](#)]
11. Frank, M.; Smetanin, S.N.; Jelínek, M.; Vyhlídal, D.; Gubina, K.A.; Shukshin, V.E.; Zverev, P.G.; Kubeček, V. Multiwavelength, picosecond, synchronously pumped, Pb(MoO<sub>4</sub>)<sub>0.2</sub>(WO<sub>4</sub>)<sub>0.8</sub> Raman laser oscillating at 12 wavelengths in a range of 1128–1360 nm. *Opt. Lett.* **2021**, *46*, 5272–5275. [[CrossRef](#)]
12. Colles, M.J. Ultrashort pulse formation in a short-pulse-stimulated Raman oscillator. *Appl. Phys. Lett.* **1971**, *19*, 23–25. [[CrossRef](#)]
13. Frank, M.; Jelínek, M.; Vyhlídal, D.; Kubeček, V.; Ivleva, L.I.; Zverev, P.G.; Smetanin, S.N. Multi-wavelength picosecond BaWO<sub>4</sub> Raman laser with long and short Raman shifts and 12-fold pulse shortening down to 3 ps at 1227 nm. *Laser Phys.* **2018**, *28*, 025403. [[CrossRef](#)]

14. Frank, M.; Smetanin, S.N.; Jelinek, M.; Vyhlidal, D.; Ivleva, L.I.; Zverev, P.G.; Kubeček, V. Highly efficient picosecond all-solid-state Raman laser at 1179 and 1227 nm on single and combined Raman lines in a BaWO<sub>4</sub> crystal. *Opt. Lett.* **2018**, *43*, 2527–2530. [[CrossRef](#)] [[PubMed](#)]
15. Granados, E.; Spence, D.J. Pulse compression in synchronously pumped mode locked Raman lasers. *Opt. Express* **2010**, *18*, 20422–20427. [[CrossRef](#)] [[PubMed](#)]
16. Ding, S.; Li, H.; Che, X.; Peng, S. Numerical analysis of synchronously pumped solid-state Raman lasers. *Opt. Express* **2020**, *28*, 35251–35263. [[CrossRef](#)] [[PubMed](#)]
17. Isaev, S.K.; Kornienko, L.S.; Kravtsov, N.V.; Serkin, V.N. Formation of ultrashort light pulses in a laser with a bleachable filter by intracavity generation of Raman emission. *Sov. J. Quantum Electron.* **1981**, *11*, 365–370. [[CrossRef](#)]
18. Pershin, S.M.; Shashkov, E.V.; Vorobiev, N.S.; Nikitin, S.P.; Grishin, M.Y.; Komel'kov, A.S. Asymmetric broadening and blue shift of the stimulated Raman scattering spectrum in water under chirped picosecond laser pulse train excitation. *Laser Phys. Lett.* **2020**, *17*, 115403. [[CrossRef](#)]
19. Babushkin, A.V.; Vorob'ev, N.S.; Prokhorov, A.M.; Shchelev, M.Y. Stable picosecond YAlO<sub>3</sub>:Nd crystal laser with hybrid mode locking and passive intracavity feedback utilizing a GaAs crystal. *Sov. J. Quantum. Electron.* **1989**, *19*, 1310–1311. [[CrossRef](#)]
20. Zubko, A.E.; Shashkov, E.V.; Smirnov, A.V.; Vorobiev, N.S.; Smirnov, V.I. On the use of a chirped Bragg grating as a cavity mirror of a picosecond Nd: YAG laser. *Quantum Electron.* **2016**, *46*, 147–149. [[CrossRef](#)]
21. Maxwell, T.; Ruan, J.; Piot, P.; Lumpkin, A. Synchronization and characterization of an ultrashort pulse laser for photoemission and electron-beam diagnostics at a radio frequency photoinjector. *J. Instrum.* **2012**, *7*, T11001. [[CrossRef](#)]
22. Vorobiev, N.S.; Gornostaev, P.B.; Lozovoi, V.I.; Smirnov, A.V.; Shashkov, E.V.; Schelev, M.Y. A PS-1/S1 picosecond streak camera in experimental physics. *Instrum. Exp. Tech.* **2016**, *59*, 551–556. [[CrossRef](#)]
23. Grigoryan, G.G.; Sogomonyan, S.B. Synchronously pumped picosecond Raman laser utilizing an LiIO<sub>3</sub> crystal. *Sov. J. Quantum Electron.* **1989**, *19*, 1402–1404. [[CrossRef](#)]
24. Bespalov, V.I.; Pasmanik, G.A. Stimulated Mandel'shtam-Brillouin and entropy backscattering of light pulses. *Sov. Phys. J. Exp.* **1970**, *31*, 168–174.